Advanced Ceramics Progress: Vol. 8, No. 1, (Winter 2022) 18-26

Materials and Energy Research Center
MERC

Contents lists available at ACERP

Advanced Ceramics Progress

Journal Homepage: www.acerp.ir

Original Research Article

Evaluating the Effect of the Constituent Content on the Mechanical and Biological Properties of Gelatin/Tragacanth/Nano-Hydroxyapatite Scaffolds

Parisa Madani [a], Saeed Hesaraki [b,*], Maryam Saeidifar [c], Navid Ahmadi Nasab [d,e]

[a] *PhD Candidate, Department of Nanotechnology and Advanced Materials, Materials and Energy Research Center (MERC), Meshkindasht, Alborz, Iran*

[b] *Professor, Department of Nanotechnology and Advanced Materials, Materials and Energy Research Center (MERC), Meshkindasht, Alborz, Iran*

[c] *Associate Professor, Department of Nanotechnology and Advanced Materials, Materials and Energy Research Center (MERC), Meshkindasht, Alborz, Iran*

[d] *Assistant Professor, Department of Marine Biology, Faculty of Marine Science and Technologies, University of Hormozgan, Bandar Abbas, Hormozgan, Iran*

[e] *Assistant Professor, Hormoz Research Center, University of Hormozgan, Bandar Abbas, Hormozgan, Iran*

* Corresponding Author Email: s-hesaraki@merc.ac.ir (S. Hesaraki)

URL: https://www.acerp.ir/article_150699.html

ARTICLE INFO

Article History:

Received 23 April 2022
Received in revised form 21 May 2022
Accepted 31 May 2022

Keywords:

Gelatin
Tragacanth
Nano-Hydroxyapatite
Bone
Mechanical Properties

ABSTRACT

Scaffolds made of three components containing Gelatin (30.3-64.7 wt. %), Tragacanth (23.5-60.6 wt. %) and nano-Hydroxyapatite (9.09-11.67 wt. %) were fabricated through the freeze drying process. Among the scaffolds with the components in the mentioned range, three scaffolds were selected for comparison based on pre-test steps including washout and soaking in SBF for 28 days to evaluate their consistency. At the end, two scaffolds with the maximum and moderate wt. % of gelatin were selected for further studies. The same pre-tests were done to select one of the cross-linkers namely GPTMS, $CaCl_2$, and Glutaraldehyde. As a result, GPTMS with the total amount of 10 % of the total polymers wt. % was selected as the cross-linker. The mechanical properties of the scaffolds were investigated through the compressive test, and the one with higher Gelatin content had the highest Elastic modulus. In addition, the biodegradability of the scaffolds was studied by soaking them in the PBS for 1, 3, 7, 14, 21, and 28 days and measuring the weight loss. Higher contents of Gelatin resulted in less degradation. In this research, the biocompatibility of the samples was surveyed by soaking them in the SBF for 1, 3, 7, 14, 21, and 28 days, and the formation of the apatite layer on the scaffold surface was studied using the XRD, FTIR, and SEM techniques. Of note, the apatite layer can be finely formed on the sample with moderate Gelatin content. Other two scaffolds with the maximum and minimum Gelatin contents were completely deteriorated in the SBF.

https://doi.org/10.30501/acp.2022.338756.1087

1. INTRODUCTION

Bone is a highly vascularized tissue that is able to remodel itself to maintain skeletal integration. However, in some cases, when bone loses this ability, bone mass loss and osteoporosis would occur. One of the major

Please cite this article as: Madani, P., Hesaraki, S., Saeidifar, M., Ahmadi Nasab, N., "Evaluating the Effect of the Constituent Content on the Mechanical and Biological Properties of Gelatin/Tragacanth/Nano-hydroxyapatite Scaffolds", ***Advanced Ceramics Progress***, Vol. 8, No. 1, (2022), 18-26. https://doi.org/10.30501/acp.2022.338756.1087

causes of osteoporosis is the lack of balance between the osteoblast and osteoclast activities that cause bone formation and bone resorption, respectively, hence a decrease in the bone mass and its vulnerability against trauma. Traditional therapies such as bone autografts, in addition to being invasive, may cause some problems such as infection. Given the considerable advantages of bone tissue engineering methods including low costs, less trauma, and immunotoxicity, they have drawn a great deal of attention due to their different applications. For instance, bone tissue engineering scaffolds have been widely used in the past few years in order to prevent the progression of osteoporosis and treat the damages to the bone. These scaffolds are required to have some physical and mechanical properties similar to those of bones namely the bioactivity, biocompatibility, non-toxicity, and cell attachment to stimulate bone formation [1]. Given that the damaged and porous bones are less able to remodel themselves, there are only a few cases of bone tissue engineering scaffolds that have succeeded in bone remodeling. Therefore, choosing the proper components of the bone tissue engineering scaffold and determining the ratio of the components are the major challenges in this regard. Since the natural bone is composed of organic and inorganic nano-composites, the elemental texture of the bone is stiff, mainly containing inorganic calcium hydroxyapatite with the chemical formula of $Ca_{10}(PO_4)_6(OH)_2$ as Nano-crystals, which is the main causes of bone stiffness. The organic phase of the bone matrix is mainly composed of Type I collagen which is an elastic protein that optimizes fracture strength and strengthens the attachment, growth, and differentiation cells. Other organic components existing in the bone tissue are glycosaminoglycans, osteocalcin, osteonectin, bone sialoproteins, and osteopontin. Despite the high strength of the inorganic matrix of the bone, it is still fragile. On the contrary, the organic matrix (like Collagen fibrils) is flexible yet less strong. The combination of these two phases form a matrix with high strength and flexibility that is not brittle.

Since the bone matrix is made of different components with the mentioned properties, the tissue engineering scaffolds designed to mimic the bone behaviors and properties must be composed of different ingredients. Therefore, choosing the best materials for fabricating the bone tissue engineering scaffold is an improtant challenge to be taken into account. In addition, the weight percentage of the scaffold components is another factor that affects the scaffold function when used in bones with osteoporosis or trauma. The currsent study put its main focus on these two challenges in order to design and fabricate a scaffold used in non-load bearing bones or bones with osteoporosis issues.

The main constituent of the scaffold in this study is Gelatin which is a natural polymer that can mimic extracellular matrix and provide a convinient microenvironment for cell growth and proliferation [2] since it is composed of amino acids and peptides obtained from minor hydrolysis of triple helix bonds of Collagen. Among these amino acids, Arginine, Glycine, and Aspartic acid (RGD sequence) provide the necessary signals for the proliferation, adhesion and differentiation of cells. However, Gelatin has high degradation rate and low compressive strength of about 0.03 MPa, hence not suitable for bone tissue engineering applications. Therefore, Gelatin must be utilized in a combination with other components such as chitosan, hyaloronic acid or collagen (proteins and polysaccharids) which are used in several bone tissue engineering applications due to their proper degradation rate and less immunological responses [3]. Among these natural biopolymers, polysaccharids, specifically natural gums, have significantly drawn attention due to their availability, low preparation costs, hydrophilicity, appropriate biological responses, resembling extracellular matrix properties, and high binding capability [4].

One of these natural gums is Gum Tragacanth (GT) which is a heterogeneous branched anionic polysaccharid obtained from a native Iranian herb that simulates bone features in the scaffold [5]. It is an antibacterial polymer with high molecular weight that is easily solved or well dispersed in water. It is also highly resistant against heat, acidity, and aging. It has been proved that using GT-based hydrogels would increase osteoconductivity, compared to Collagen hydrogels and tissue culture plate. Tragacanth is a non-toxic material with the highest ALP activity and bone mineralization with the highest expression of Runx-2, osteonectin, and osteocalcin by the bone mesenchymal stem cells, which are the main factors contributing to bone formation and osteogenic differentiation. GT also plays a key role as a binder that helps omit toxic crosslinkers [6]. Moreover, adding it to the common matrices used for encapsulation of bone cells used in bone tissue engineering such as Calcium Alginate (CA) beads improves degradation and swelling of the beads and stimulates cell proliferation and differentiation. Due to the abundant hydroxyl (OH) and carboxyl (COOH) groups existing in the GT, it provides suitable sites for crosslinking and Hydrogen binding with other molecules with the same functional groups [7]. Of note, the presence of active functional groups in the GT chains as the binding sites is another notable characteristic of this gum that makes it suitable for conjuction of drugs. In addition, its swelling ability, which creates a three dimensional network, makes it a proper choice for drug encapsulation that turns it into a desirable drug delivery system [8]. Moreover, GT is anti-microbial, anti-inflammation, non-allergic, and non-toxic [9]. Despite all these high-grade properties of GT, this gum have been limitedly applied in bone tisssue engineering and osteogenesis. For this reason, this constituent is a novel component of the scaffold in this study. Osteogenic differentiation of human adipose-derived mesenchymal stem cells cultured on the GT

hydrogel was already proved, thus confirming its application in orthopedics and bone regeneration [10].

In order to utilize this polysaccharide in bone tissue engineering, its structure must be stabilized using biocompatible coupling agents and crosslinkers such as GPTMS (3-glycidoxypropyl) [11]. Not only does this crosslinker increase the consistency of this biopolymer, but also it adjusts its biological properties and optimizes the interfacial interactions of the composites containing GT [12,13]. GPTMS is biologically safe and non-toxic and that facilitates cell adhesion and proliferation.

Although fabrication of a bone tissue engineering scaffold with only two polymer consituents simulates the organic phase of the extracellular matrix and results in cell ingrowth, the bioactive components are still necessary for bone healing. Among these components is Hydroxyapatite (HAp) which is the most important inorganic component of the natural bone that is highly bioactive and non-toxic [14,15]. HAp can improve the mechanical properties of the scaffold and increase both cell proliferation and adhesion by creating hydrophilic surfaces [15]. It also enhances the osteogenic differentiation of the mesenchymal stem cells. In addition, it has good distribution, thus facilitating the interactions between the scaffold and osteogenic cells owing to the relatively high ratio of the surface area to volume.

In order to design a scaffold with the mentioned properties, we must determine the ratio of the scaffold components as well. In this study, attempts were made to design a scaffold with three components and determine the best wt. % of the components in order to obtain the best mechanical and biological properties. To this end, three scaffolds with different wt. % of the components containing Gelatin, Nano-HAp, and Tragacanth were designed to choose the best scaffold with the closest mechanical properties to those of the cortical bone, fine apatite formation, and same biodegradability rate as the cortical bone formation.

In fact, the main objective of this study was to design and fabricate a scaffold simulating cortical bone mechanical, physical, and biological properties based on the interactions among the components.

2. MATERIALS AND METHODS

2.1. Starting Materials

In order to prepare the scaffold, Nano-HAp (CAS 12167-74-7) with the particle size of < 200 nm, Gelatin Type B (obtained from alkaline hydrolysis of insoluble Collagen) from bovine skin, Tragacanth, G1128, (CAS 9000-65-1, EC 232-552-5), and Glutaraldehyde (CAS 111-30-8) were purchased from SIGMA-Aldrich, Germany. In addition, Calciumchlorid (CAS 10043-52-4) and GPTMS (CAS 2530-83-8) were purchased from Merck, Germany and then, Phosphate-Buffered Saline (PBS) with 1X concentration and pH of 7.3 (CAS 11510546) was purchased from Gibco, United Kingdom. Double Distilled (DD) water was used as the solvent for the scaffold components, and SBF was prepared based on the Kokubo method [16].

2.2. Composition of the Scaffolds

In this study, different compositions of the scaffolds were investigated to find the best scaffold with the optimum mechanical, physical, and in vitro biological properties.

As a result, three scaffolds were designed considering the following compositions given in Table 1. All the compositions were inserted as wt. %, and their compositions were designed according to our pre-tests, containing wash out with DD water and soaking in SBF for 28 days. Samples that were not completely deteriorated in the SBF for 28 days were selected for further studies. All the ratios of GPTMS, the crosslinking agent, were constant. The total amount of the cross-linking agent was considered 10 % of the total weight of the polymers used. Of note, GPTMS was selected as the cross-linking agent according to the pre-tests when compared to $CaCl_2$ and Glutaraldehyde mainly because the scaffolds fabricated with different percentages of the other two cross-linkers were washed out in distilled water and completely deteriorated in the SBF solution after one day. It is worth mentioning that the scaffold with the minimum wt. % of Gelatin was deteriorated in the washing process with DD water and therefore, it was omitted. Finally, only two scaffolds with maximum and moderate wt. % of Gelatin remained, hence selected for further studies.

TABLE 1. Compositions of the studied scaffolds

Composition	Gelatin	Tragacanth	nHAp	GPTMS
G1	30.3 %	60.6 %	9.09 %	Fixed
G2	47.5 %	42.05 %	10.42 %	Fixed
G3	64.7 %	23.5 %	11.76 %	Fixed

2.3. Scaffolds Fabrication Technique

Solutions of the scaffold components with equal volumes and different wt. % of the components were prepared. In order to make G1, first, 0.909 g of nHAp was poured into 10 cc of distilled water and mixed on a stirrer to obtain a homogeneous solution. Then, 3.03 g of Gelatin was poured into 10 cc of distilled water. Given the better solulabilituy and more uniformity of gelatin at higher temperatures, the obatined solution was transferred to a heater-stirrer at the temprature of 40-50 °C and mixed for 30 minutes to be completely dissolved. Afterwards, 6.06 g Tragacanth was added to 10 cc of distilled water and mixed with a heater-stirrer to be uniformly dissolved. GPTMS was then added to the gelatin solution and mixed for another 30 minutes. All

mixing processes were done at the speed of 350 rpm. The total amount of GPTMS was considered as 10 % of the total weight of the polymers: (3.03+6.06)*10% = 0.9. Subsequently, 0.9 cc of GPTMS was added to the gelatin solution. These three aqua solutions were incorporated and mixed for 24 hours on a heater-stirrer at the temparature and mixing speed of 40 °C and 350 rpm, respectively. The acquired solution was poured into 3 cc syringes, transferred to the liquid Nitrogen for quick freezing, kept aways from percipitation of nHAp particles, and kept in a -20 °C freezer overnight mainly because nHAp would only be dispersed in the composition. The obtained cylindrical structure was then put in the freeze dryer (Pishtaz Equipment Engineering Co.) for 48 hours to complete the scaffold fabrication procedure.

The same process was repeated for G2 and G3 scaffolds with the mentioned wt. % of the components.

2.4. Experiments

To study the mechanical properties, biocompatibility, degradation rate, and cell attachment, the following experiments were carried out.

2.4.1. Mechanical Testing

The scaffolds were cut into cylindrical shapes with the diameter and height of 10 mm and 20 mm, respectively, with parallel surfaces. The specimens were then transferred to a compressive strength testing device (SANTAM STM-20). Compression tests were repeated with three samples for each scaffold, and the Elastic modulus of the scaffolds were obtained through the following equation:

$$E = \sigma(\varepsilon)/\varepsilon = \frac{F/A_\circ}{\Delta L/L_\circ} = \frac{FL_\circ}{A_\circ \Delta L} \quad (1)$$

2.4.2. Physical Characterizing

The scaffolds were characterized using FTIR, XRD, and SEM prior to and followed by soaking in the SBF solution at different time intervals of 3, 7, 14, 21, and 28 days to evaluate the phases and bonds and make sure whether the bonds between the three components are made and they are crosslinked as well and also, to study the apatite formation in order to evaluate biocompatibility of the scaffolds. The samples were also studied using the Scanning Electron Microscopy (SEM) to monitor their structure and porosity.

2.4.3. In vitro Apatite Formation

Scaffolds used in the non-load bearing bone defects must be attached well to the adjacent bone. This process is not done unless a proper layer of apatite is formed on the surface of the scaffold. In this regard, the apatite layer formation test in Simulated Body Fluid (SBF) was done.

Scaffold cylindrical samples were submerged in the SBF solution for 3, 7, 14, 21, and 28 days. All FTIR, XRD, and SEM experiments were carried out to find information about the chemical composition of the surface, figure out whether or not the apatite layer is formed, and measure the thickness of the apatite layer.

2.4.3.1. FTIR

To prepare the samples for the FTIR spectroscopy (Victor 33, Broker, Germany) with 45 scan per sample, the scaffolds were first grinded, and the obtained powder was mixed with Potassium Bromide (KBr, an inactive material against the IR spectra) to acquire powder particles with the diameters of less than 2 µm. Then, the powder was compressed to obtain shots and exposed to IR spectra to record the FTIR spectra.

Apatite formation was also evaluated using FTIR analysis for the scaffolds prior to and followed by soaking in SBF for 28 days based on a comparison between the obtained spectrum and identified peaks related to Carbonated HAp.

2.4.3.2. SEM

The scaffolds were cut into thin slices with the dimensions of 3 mm, dried well, and covered with a thin layer of gold in order to make them electro-conductive. Then, the samples were placed into the SEM S360-Cambridge 1990, and the obtained images were analyzed to investigate apatite formation on top of the scaffolds. The images were compared for the scaffolds before and after 28 days of simmering in SBF.

2.4.3.3. XRD

The XRD pattern of the scaffold was obtained using Philips PW3710 diffractometer with the X-Ray source of Cu-Kα and step size of 0.02°. It is worth mentioning that λ was obtained as 0.154 nm.

2.4.4. In vitro Biodegradation

Scaffolds were soaked in Phosphate Buffer Saline (PBS) for 3, 7, 14, 21, and 28 days. Then, their weight changes were evaluated.

3. RESULTS AND DISCUSSION

3.1. Mechanical Testing

Since the fabricated scaffolds are meant to be placed in the cortical bones and preferably in non-load bearing sites, their mechanical properties were evaluated using compression test (SANTAM STM-20) at the speed of 1 mm/min. All compression tests were repeated with three samples, and the mean value of their mechanical properties was considered as the result.

Figure 1 shows the elongation of the samples as a function of the applied force for the G2 sample. The elastic modulus as long of peak for each sample was 1.67,

1.31, and 1.39 MPa, and the average Elastic modulus was 1.456 MPa. All mean values of the other mechanical properties related to the samples of G2 and G3 are shown in Table 2. Elongation as a function of force for the G3 sample is given in Figure 2. The compression test was repeated with three samples.

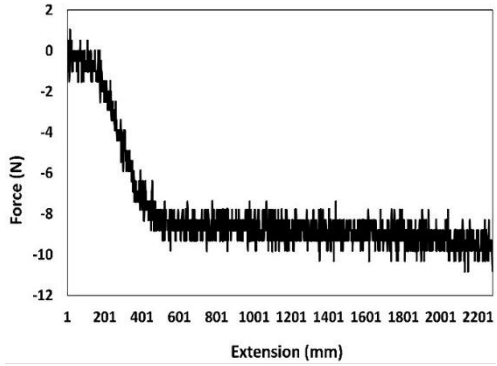

Figure 1. Elongation as long of peak for the G2 sample

TABLE 2. Mean values of the mechanical properties of the G2 and G3 samples

	G2		G3	
Sample	Peak	Break	Peak	Break
Force (N)	-10.8	-10.3	-54	-52.7
Extension (mm)	-5.94	-5.94	-6.04	-6.08
Stress (MPa)	-0.25	-0.23	-1.13	-1.12
Elongation (%)	-43.4	-43.4	-42.27	-42.58
Elong Aft. Brk (%)	-25.15	-26.01	-32.27	-32.68
Energy (J)	-30.6	-30.57	-159.83	-159.5
Bending St. (MPa)	-0.87	-0.83	-4.17	-4.13
Bending Strain	-1.45	-1.45	-1.38	-1.4
Bending Module	0.61	0.58	3.04	2.98

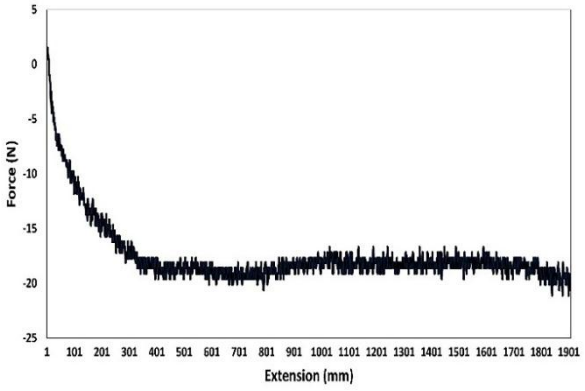

Figure 2. Elongation as long of peak for the G3 sample

According to the results, the mean elastic modulus for the G2 scaffold and the G3 scaffolds were 1.4 MPa and 12.47 MPa, respectively. The elastic modulus of the G2 scaffold is lower than those of the other due to less Gelatin wt. %.

Given that the main crosslinking occurs mostly between Gelatin, Tragacanth, and GPTMS, less wt. % of these two components would result in less crosslinking and lower strength of the scaffold, thus confirming the results from the previous studies emphasizing that Gelatin and GT acted as the binder in ceramic scaffolds [17].

Higher wt. % of nHAP is another reason for higher elastic modulus of the G3 scaffold. To be specific, according to the previous studies [18], an increase in the wt. % of HAp results in higher elastic modulus, which is an outcome of higher scaffold integrity due to less porosity. Higher wt. % of GT in the G2 samples results in higher compression yield strength and compressive strength, and a decrease in the porosity, according to the previous studies [10]. However, higher wt. % of Gelatin and its effect on mechanical properties undermined the role of wt. % of GT in the scaffold.

Based on the results from the mechanical testing, it can be concluded that the G3 sample has closer elastic modulus to that of the trabecular bone, which is in the range of 10-3000 MPa. However, given that the elastic modulus of the trabecular bone decreases by 10 % for every decade of aging due to the changes in the bone density and increase in the anisotropy of bone compressive strength, the G2 sample can be technically a better choice for bone remodeling throughout the healing process based on the tissue engineering approaches. Moreover, damages casued by osteoporosis can have the same effect on the cancellous bone. As a result, the scaffold has less elastic modulus and less compressive strength, hence a better choice for cortical bone substitute. Of note, the compressive strength of the spongy bone is quite low, i.e., approximately 0.036-2.945 MPa [10].

3.2. Physical Characterizing

3.2.1. In vitro Biodegradation

Scaffolds were soaked in the PBS for 3, 7, 14, 21, and 28 days and changes in their weights were evaluated. The degradation value can be obtained through the following formula:

$$\text{Degradation}= \frac{m2-m1}{m1} *100 \quad (2)$$

where m_2 is the sample weight after its exposure to the PBS, and m_1 the initial weight of the sample. Figure 3 refers to the degradation as a function of time for G2 and G3 samples.

According to the degradation results, the degradation percentage increased with time for both sample groups, and the degradation rate of the G2 sample after 28 days was more than that of the other samples mainly because of the lower wt. % of Gelatin and GT since more cross-linking happens between Gelatin, GT, and GPTMS, and G2 has lower wt. % of these two components.

Both G2 and G3 scaffolds were characterized by fair biodegradability as well as 10.3 % and 9.5 % weight loss after 28 days soaking in the PBS, respectively. This is a fair degradation rate because the first two stages of bone remodeling, i.e., resorption and reversal, takes about six to seven weeks to be completed, and the last stage, i.e., bone formation, takes up to four months to completely heal the bone [19].

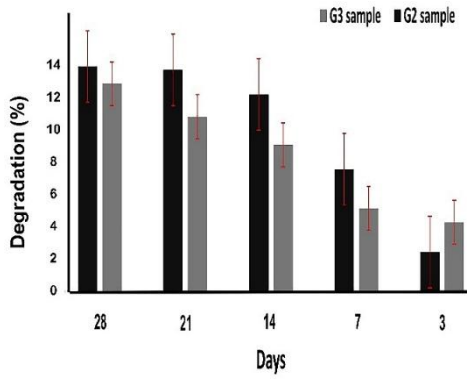

Figure 3. Degradation percentage for the scaffolds in the PBS at different time intervals

Higher weight loss of the G2 sample can be attributed to lower wt. % of nHAP and Gelatin. As stated in the previous studies [16], higher amounts of nHAP would result in less porosity and consequently less degradation due to less diffusion of the PBS into the scaffold. Further, higher wt. % of gelatin in the G3 sample nullified the binding effect of higher wt. % of Tragacanth in the average sample, thus resulting in lower degradation rate. Two or three weeks after the trauma marks the beginning of the transformation of a fragile cartilage like tissue in the defect site into the bone tissue. This process takes about 6 to 12 weeks (6 weeks for the upper limb, and 12 weeks for the load-bearing sites). In fact, since the degradation rate of the scaffolds were close, the G2 scaffold was selected as the optimum one owing to the other properties similar to the cortical bone.

3.2.2. In vitro Apatite Formation

3.2.2.1. SEM Analysis

SEM images from the samples prior to and followed by soaking in the SBF were compared to study whether or not the apatite layer was formed. After 28 days of soaking in the SBF, the G3 sample was completely deteriorated, and the apatite formation was monitored after three days. Then, the G2 samples were dried at the room temperature, cut into thin slices with the dimensions of 3 mm, and covered with a thin layer of gold to make the samples electro-conductive. Next, the samples were put inside the SEM (SEM S360-Cambridge 1990).

Figures 4-7 depcit the SEM images of both sample groups where the apatite layer is clearly visible as the lighter areas. A thick and dense layer of apatite was finally formed on the G3 sample surface, and the porosity of the sample was reduced due to shrinkage caused by higher wt. % of Gelatin.

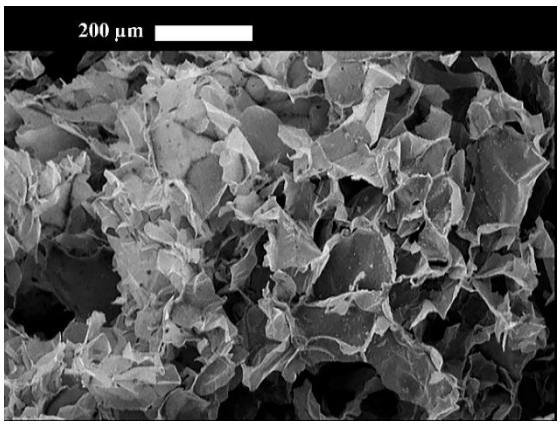

Figure 4. SEM image of the G2 sample before soaking in the SBF

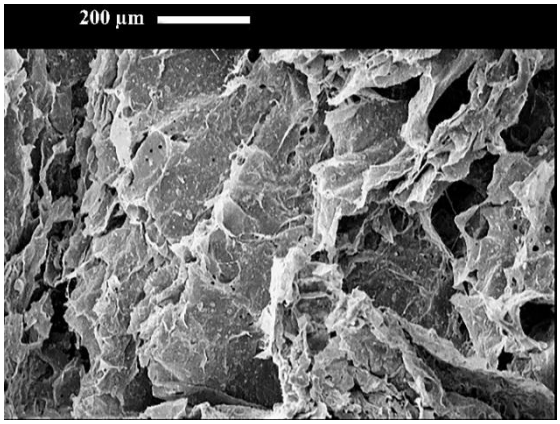

Figure 5. SEM image of the G2 sample after soaking in the SBF for 28 days. Carbonared Nano-HAp percipitates are visible

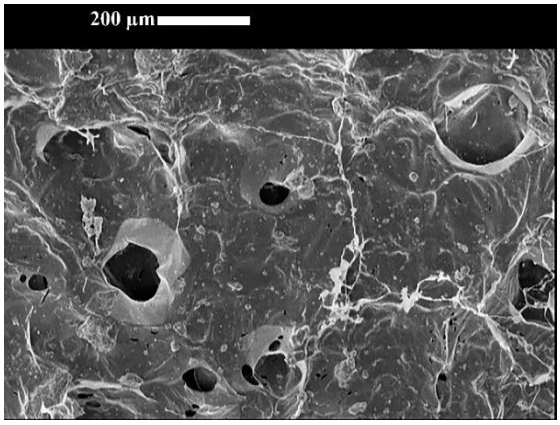

Figure 6. SEM image of the G3 sample before soaking in SBF

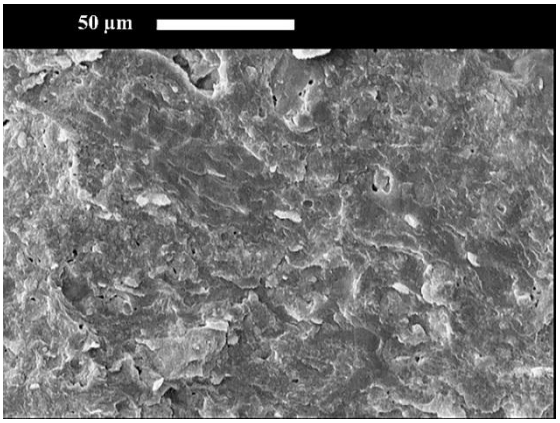

Figure 7. The SEM image of the G3 sample after soaking in the SBF for three days. Carbonated Nano-HAp percipitates are visible

3.2.2.2. XRD Analysis of the Scaffolds

Figures 8 and 9 show the XRD patterns of the G2 and G3 scaffolds, respectively, prior to and followed by soaking in the SBF for 28 days. Given that the G3 scaffold was deteriorated in the SBF after one day, the XRD pattern was obtained only before soaking in the SBF. As indicated in both XRD patterns, a sharp peak around 2θ=32° is observed corresponding to the carbonated HAp for the (211) and (112) atomic planes (according to JCPDS-9-432) which broadens after soaking in the SBF, and the peak width is reduced which is a sign of crystallization of the Carbonated HAp.

3.2.2.3. FTIR Analysis of the Scaffolds

Since the G3 sample was deteriorated in the SBF, its FTIR spectra was obtained only before soaking in the SBF, as shown in Figure 10.

Table 3 confirms the presence of the peaks and their corresponding bonds of the G3 sample.

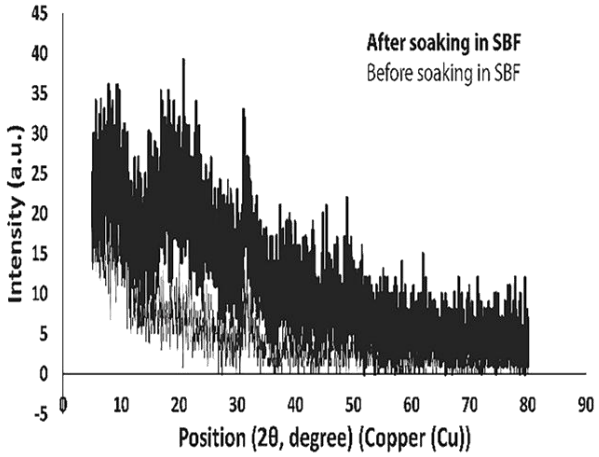

Figure 8. XRD pattern of the G2 sample before and after 28 days soaking in SBF

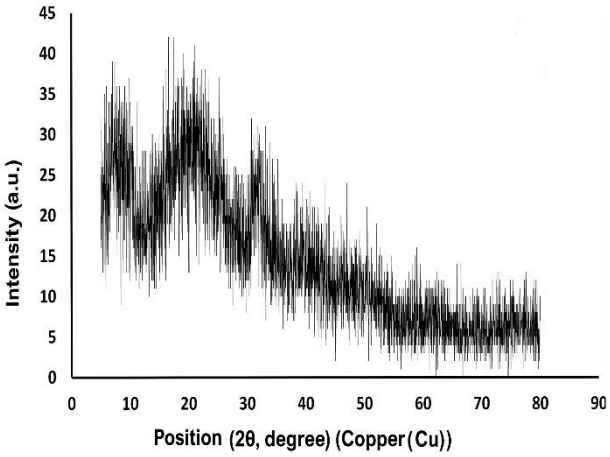

Figure 9. XRD pattern of the G3 sample before and after 28 days soaking in SBF

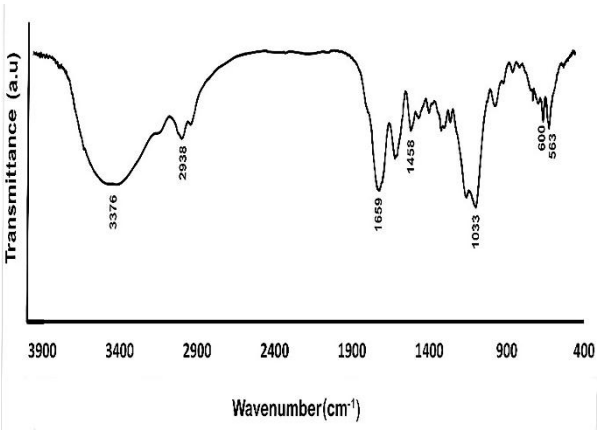

Figure 10. FTIR spectra of the G3 scaffold

TABLE 3. Peaks of FTIR spectra for the G3 sample

Wave No.	Stretching Mode	Ref.
3376	Stretching vibration of O-H groups in Gum Tragacanth	[20]
2938	Symmetric stertching vibrations of methylene groups in Gum Tragacanth	[20]
1659	Amide I regions in Gelatin containing C=O stretching vibration with contribution of C-N bond stretching vibration	[21]
1458	Asymmetric stretching of CO_3^{2-} in nHAp	[22]
1033	Asymmetric stretching of PO_4^{3-} in nHAp	[22]
600	Amide III region in Gelatin representing vibration in the plane of C-N and N-H groups of bound amide or vibration of CH_2 groups	[21]
563	Asymmetric bending vibration of PO_4^{3-} in nHAp	[22]

Table 4 shows the peaks of the FTIR spectra of the G2 sample.

TABLE 4. Peaks of FTIR spectra for the G2 sample

Wave No.	Stretching Mode	Ref.
3345	Stretching vibrations of O–H groups in the gum Tragacanth	[20]
2935	Symmetric stretching vibrations of methylene groups in the gum Tragacanth	[20]
2880	Asymmetric stretching vibrations of methylene groups in Gum Tragacanth	[20]
1662	C–O stretching vibrations of polyols vibration with contribution of C-N bond stretching vibration in Amide I regions of Gelatin	[21]
1551	Amide II regions in Gelatin from N-H bending vibration and C-N stretching vibration	[21]
1454	Ion Stretching of O-H in nHAp	[22]
1240	C–O stretching vibrations of polyols in Gum Tragacanth	[20]
1204	vibration in the plane of C-N and N-H groups of bound amide or vibration of CH2 group in Amide III region of Gelatin	[21]
1092	Asymmetric stretching of PO_4^{3-} in nHAp	[22]
918	Out of plane bending mode CO_3^{2-} in nHAp	[22]
598	Asymmetric bending vibration of PO_4^{3-} in nHAp	[22]
563	Asymmetric bending vibration of PO_4^{3-} in nHAp	[22]

Figure 11 makes a comparison between the FTIR spectra of the G2 sample prior to and followed by soaking in the SBF based on which, it can be concluded that the apatite already began to crystallize since the twin peak at 1092 cm^{-1} in the G2 sample was turned into a single peak. Peaks at around 1400 cm^{-1} are related to Carbonates, and the twin peaks at 1415 cm^{-1} in the sample after soaking is indicative of the Carbonated HAp.

A decrease in the peak intensity at 2940 cm^{-1} in the sample after soaking, compared to that at 2935 cm^{-1} in the sample before soaking which is related to the C-H bonds, shows that the polymer components of the scaffold were absorbed, meaning that the scaffold is being well-degraded.

Moreover, the peak at 1546 cm^{-1} in the spectra followed by soaking is also attributed to the carbonated HAp, and the peaks at 601 and 563 cm^{-1} are attributed to PO_4^{3-}.

Elimination of the peaks at 1240 and 1204 cm^{-1} wavenumbers in the FTIR spectra of the G2 scaffold after soaking in SBF is a sign of polymeric regions of the scaffold since these two wavenumbers are related to GT and Gelatin, respectively.

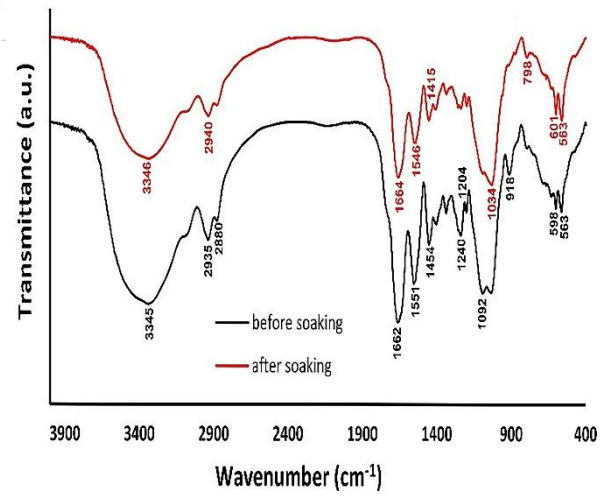

Figure 11. FTIR spectra of the G2 scaffold prior to and followed by soaking in SBF for 28 days

4. CONCLUSION

The current research primarily aimed to design and fabricate three scaffolds with different wt. % components namely Gelatin, Tragacanth, and Nano-HAp. At the end of the study, based on the mechanical, physical and biological experiments, the G2 scaffold, the sample with the moderate wt. % of Gelatin (The scaffold containing 47.5 % Gelatin, 42.05 % Tragacanth, and 10.42 % nHAp), was selected as the optimum sample for bone tissue engineering. The Elastic modulus of this scaffold was measured as 1.45 MPa, which was suitable for spongy or defected bones with osteoporosis. The apatite formation of the mentioned scaffold was proved and investigated using the XRD, FTIR, and SEM analyses. As observed in the SEM images, the apatite layer are clearly visible, and the peaks in the XRD spectra at $2\theta=32°$ demonstrate the carbonated HAp, the main component of the natural bone. Differences in the peak intensities of the FTIR spectra priror to and followed by soaking in the SBF were indicative of the apatite crystalization and polymer components absorption as a result of the scaffold degradation. These results in general proved that the scaffold designed and fabricated in this study could be a promising one for further bone tissue engineering studies.

ACKNOWLEDGEMENTS

The authors would like to acknowledge Mr. Nouraie and Kavousi, the XRD and FTIR lab. Managers.

REFERENCES

1. Feng, P., He, J., Peng, S., Gao, C., Zhao, Z., Xiong, S., Shuai, C., "Characterizations and interfacial reinforcement mechanisms of multicomponent biopolymer based scaffold", ***Materials Science and Engineering: C***, Vol. 100, (2019), 809-825. https://doi.org/10.1016/j.msec.2019.03.030
2. Ma, P., Wu, W., Wei, Y., Ren, L., Lin, S., Wu, J., "Biomimetic gelatin/chitosan/polyvinyl alcohol/nano-hydroxyapatite scaffolds for bone tissue engineering", ***Materials & Design***, Vol. 207, (2021), 109865. https://doi.org/10.1016/j.matdes.2021.109865
3. Hesaraki, S., Nouri-Felekori, M., Nezafati, N., Borhan, S., "Preparation, characterization, and in vitro biological performance of novel porous GPTMS-coupled tragacanth/nano-bioactive glass bone tissue scaffolds", ***Materials Today Communications***, Vol. 27, (2021), 102335. https://doi.org/10.1016/j.mtcomm.2021.102335
4. Wubneh, A., Tsekoura, E.K., Ayranci, C., Uludağ, H., "Current state of fabrication technologies and materials for bone tissue engineering", ***Acta Biomaterialia***, Vol. 80, (2018), 1-30. https://doi.org/10.1016/j.actbio.2018.09.031
5. Shafiee, S., Ahangar, H. A., Saffar, A., "Taguchi method optimization for synthesis of Fe_3O_4@ chitosan/Tragacanth Gum nanocomposite as a drug delivery system", ***Carbohydrate Polymers***, Vol. 222, (2019), 114982. https://doi.org/10.1016/j.carbpol.2019.114982
6. Hajinasrollah, K., Habibi, S., Nazockdast, H., "Fabrication of gelatin–chitosan–gum tragacanth with thermal annealing cross-linking strategy", ***Journal of Engineered Fibers and Fabrics***, Vol. 14, (2019), 1558925019881142. https://doi.org/10.1177%2F1558925019881142
7. Apoorva, A., Rameshbabu, A. P., Dasgupta, S., Dhara, S., Padmavati, M., "Novel pH-sensitive alginate hydrogel delivery system reinforced with gum tragacanth for intestinal targeting of nutraceuticals", ***International Journal of Biological Macromolecules***, Vol. 147, (2020), 675-687. https://doi.org/10.1016/j.ijbiomac.2020.01.027
8. Singh, B., Sharma, K., Dutt, S., "Dietary fiber tragacanth gum based hydrogels for use in drug delivery applications", ***Bioactive Carbohydrates and Dietary Fibre***, Vol. 21, (2020), 100208. https://doi.org/10.1016/j.bcdf.2019.100208
9. Mohammadi, M. R., Kargozar, S., Bahrami, S. H., Rabbani, S., "An excellent nanofibrous matrix based on gum tragacanth-poly (ε-caprolactone)-poly (vinyl alcohol) for application in diabetic wound healing", ***Polymer Degradation and Stability***, Vol. 174, (2020), 109105. https://doi.org/10.1016/j.polymdegradstab.2020.109105
10. Lett, J. A., Sundareswari, M., Ravichandran, K., Latha, B., Sagadevan, S., "Fabrication and characterization of porous scaffolds for bone replacements using gum tragacanth", ***Materials Science and Engineering: C***, Vol. 96, (2019), 487-495. https://doi.org/10.1016/j.msec.2018.11.082
11. Rasti, M., Hesaraki, S., Nezafati, N., "Effects of GPTMS concentration and powder to liquid ratio on the flowability and biodegradation behaviors of 45S5 bioglass/tragacanth bioactive composite pastes", ***Journal of Applied Polymer Science***, Vol. 136, No. 22, (2019), 47604. https://doi.org/10.1002/app.47604
12. Shuai, C., Yu, L., Feng, P., Gao, C., Peng, S., "Interfacial reinforcement in bioceramic/biopolymer composite bone scaffold: The role of coupling agent", ***Colloids and Surfaces B: Biointerfaces***, Vol. 193, (2020), 111083. https://doi.org/10.1016/j.colsurfb.2020.111083
13. Nouri-Felekori, M., Khakbiz, M., Nezafati, N., Mohammadi, J., Eslaminejad, M. B., Fani, N., "Characterization and multiscale modeling of novel calcium phosphate composites containing hydroxyapatite whiskers and gelatin microspheres", ***Journal of Alloys and Compounds***, Vol. 832, (2020), 154938. https://doi.org/10.1016/j.jallcom.2020.154938
14. Chocholata, P., Kulda, V., Babuska, V., "Fabrication of scaffolds for bone-tissue regeneration", ***Materials***, Vol. 12, No. 4, (2019), 568. https://doi.org/10.3390/ma12040568
15. Yılmaz, E., Kabataş, F., Gökçe, A., Fındık, F., "Production and characterization of a bone-like porous Ti/Ti-hydroxyapatite functionally graded material", ***Journal of Materials Engineering and Performance***, Vol. 29, No. 10, (2020), 6455-6467. https://doi.org/10.1007/s11665-020-05165-2
16. Kokubo, T., Kushitani, H., Sakka, S., Kitsugi, T., Yamamuro, T., "Solutions able to reproduce in vivo surface-structure changes in bioactive glass-ceramic A-W3", ***Journal of Biomedical Materials Research***, Vol. 24, No. 6, (1990), 721-734. https://doi.org/10.1002/jbm.820240607
17. Feng, W., Enyan, G., Enmin, S., Ping, Z., Jinhua, L., "Structure and properties of bone-like-nanohydroxyapatite/gelatin/polyvinyl alcohol composites", ***Advances in Bioscience and Biotechnology***, Vol. 1, No,. 3, (2010), 185-189. https://doi.org/10.4236/abb.2010.13026
18. Razali, K. R., Nasir, N. M., Cheng, E. M., Mamat, N., Mazalan, M., Wahab, Y., Roslan, M. M., "The effect of gelatin and hydroxyapatite ratios on the scaffolds' porosity and mechanical properties", In ***2014 IEEE Conference on Biomedical Engineering and Sciences (IECBES)***, Kuala Lumpur, Malaysia, December 2014, IEEE, (2014), 256-259. https://doi.org/10.1109/IECBES.2014.7047497
19. Hadjidakis, D. J., Androulakis, I. I., "Bone remodeling", ***Annals of the New York Academy of Sciences***, Vol. 1092, No. 1, (2006), 385-396. https://doi.org/10.1196/annals.1365.035
20. Kora, A. J., Arunachalam, J|., "Green fabrication of silver nanoparticles by gum tragacanth (Astragalus gummifer): a dual functional reductant and stabilizer", ***Journal of Nanomaterials***, Vol. 2012, (2012), 869765. https://doi.org/10.1155/2012/869765
21. Pradini, D., Juwono, H., Madurani, K. A., Kurniawan, F., "A preliminary study of identification halal gelatin using quartz crystal microbalance (QCM) sensor", ***Malaysian Journal of Fundamental and Applied Sciences***, Vol. 14, No. 3, (2018), 325-330. https://doi.org/10.11113/mjfas.v14n3.942
22. Arunseshan, C., Suresh, S., Arivuoli, D., "Synthesis and characterization of nano-hydroxyapatite (n-HAP) using the wet chemical technique", ***International Journal of Physical Sciences***, Vol. 8, 32, (2013), 1639-1645. https://doi.org/10.1016/j.compositesa.2008.05.018